Combining pH-driven adsorption and photocatalysis for the remediation of complex water matrices

Carolina Cionti[1,2], Eleonora Pargoletti[1,2], Ermelinda Falletta[1,2], Claudia L. Bianchi[1,2], Daniela Meroni[1,2,*], Giuseppe Cappelletti[1,2,*]

[1]*Department of Chemistry, Università degli Studi di Milano, via Golgi 19, 20133 Milano, Italy;*
[2]*Consorzio INSTM, via Giusti 9, 50121 Florence, Italy*
**Corresponding authors: daniela.meroni@unimi.it; giuseppe.cappelletti@unimi.it*

Abstract

Water remediation by adsorption and photocatalysis present unique advantages and limitations that can make them complementary: while adsorption is a cheap and fast process that simply transfers the pollutant to another phase, photocatalysis is a slow and costly procedure that however can degrade recalcitrant pollutants. Here, we propose a sequential treatment based on reversible and selective adsorption, followed by heterogeneous photocatalysis. In particular, the reversible and selective adsorption of dye molecules was achieved by polyaniline (PANI)-based hybrid adsorbents. The role of the dye content, adsorbent dose, solution pH and electrolyte composition was investigated. By tuning the adsorption pH, an effective regeneration of the spent adsorbent could be achieved by the triggered release of the adsorbate in an aqueous solution and mild conditions. Moreover, the separation of multi-dye mixtures (methyl orange and methylene blue) was proved, also in consecutive cycles. The selective recovery of one of the components could enable dye recycling. An ensuing photocatalytic step using a commercial photocatalyst could be adopted to either degrade the leftover solution or the regeneration solution. The latter approach was here demonstrated as an example. The release of a single pollutant in aqueous solvent, with controlled composition and tunable concentration, allows performing photocatalysis more efficiently. This combined approach enables a fast and effective treatment of the effluent and an easy regeneration of the spent adsorbent with ensuing treatment of the regeneration solution for a zero-waste strategy.

Keywords

Selective adsorption; photocatalysis; sequential treatment; controlled release; polyaniline; zinc oxide

1. Introduction

Water pollution is a major issue affecting our society[1–5]. Among the largest producers of industrial wastewaters, there are textile manufacturing industries[6,7]: more than 7×10^5 tons of dyestuff are produced worldwide annually[8–11] and a daily production in an average textile mill in India consist of around 600,000 m of fabric[9,12]. Alarmingly, half of the adopted dye is likely to be present in the discharged waters[12]. Most part of the synthetic dyes are carcinogenic, highly stable organic molecules[13,14] and therefore, dye-containing effluents are a severe cause of concern for ecosystems[15–18] and human health[9,19–21].

Biological treatment, due to their cost-effectiveness, have been widely adopted in urban sewage treatment plants. However, the activity of microorganisms is hindered by high concentrations of contaminants as well as by the presence of refractory pollutants[21–24]. These limitations, along with the biological treatment complexity and duration, hamper its application in industrial effluents from textile industries. In this context, alternative strategies for improved removal of contaminants have been researched for decades[23,25].

Separation treatments, such as adsorption, can achieve a very fast and cost-effective removal of water pollutants[23,26–28], but these processes transfer the contaminants from water to another phase (usually a solid substrate)[29], which will then necessitate additional treatment and/or disposal, leaving the user with a waste to manage[30]. For instance, the most widely used adsorbents for water treatment, activated carbons, require high temperatures or toxic organic solvents to be regenerated.

On the other hand, degradation methods, such as advanced oxidation processes (AOPs), can lead to the oxidation of organic contaminants to harmless compounds[31]. Among AOPs, heterogeneous photocatalysis has proved effective in degrading a wide range of recalcitrant pollutants[32–35], but its real-world application is still limited to few pilot plants[36]. One of the main limitations of this technique lies in the long duration needed to achieve a complete pollutant degradation, with ensuing high energy costs and accumulation of hazardous reaction intermediates[37–39]. Another unsolved issue of photocatalysis is its lower efficiency in complex water matrices. It is well known that electrolytes, such as bicarbonates, can act as scavengers of the reactive radical species generated during photocatalysis, thus considerably lowering the process efficiency[40,41].

Generally, both adsorption by activated carbon and heterogeneous photocatalysis are non-selective remediation techniques. For instance, oxidizing radicals generated by photocatalysis indiscriminately attack dissolved organic species. This is generally considered an advantage as it provides a broad response to a wide range of pollutants, but it can also represent a limit. The lack of

selectivity implies that the photocatalyst does not distinguish between highly recalcitrant pollutants and quickly biodegradable compounds, unnecessarily increasing treatment costs in the case of multi-pollutant mixtures. Moreover, from a circular economy perspective, industrial wastewater should be considered as a potential source of useful chemicals to turn remediation costs into saving of raw materials. In the case of effluents from textile industries, multi-component dye mixtures, often in complex matrices, limit dye recycling. This issue could be tackled by developing reversible and selective adsorbents.

Here, we propose an integrated system based on the combination of different technologies, which has the potential to improve the general performance of wastewater treatment of dye-containing effluents. A fast, reversible and selective adsorption pre-treatment was coupled with heterogeneous photocatalysis to obtain easy recyclability of the adsorbent and a tailored advanced oxidation step. In particular, polyaniline (PANI)-based adsorbents were chosen for their environmental stability[23], high pollutant uptakes[42–45], and potential for selective adsorption due to protonation reversibility[23,46]. We adopted PANI-TiO_2 composites from a photoactivated synthesis developed by some of us[47,48], which avoids the formation of toxic and carcinogenic by-products involved in the conventional oxidative synthetic pathway. Tests performed in dye aqueous solutions showed excellent performance also in the presence of different electrolytes, high selectivity in multi-contaminant mixtures, and tunability of adsorption by modulating the pH conditions. The spent adsorbent could be easily regenerated by a fast treatment in aqueous solution and mild conditions, which releases the adsorbed dye to be then possibly recycled. A separate photocatalytic test can either be employed to degrade the leftover solution or the regeneration solution to implement a zero-waste strategy. Here we demonstrate, as an example, the second approach showing that the simplified effluent composition allows performing photocatalysis more efficiently.

2. Experimental section

All of the reagents were purchased from Merck, unless specified otherwise, and adopted without further purification. Solutions and suspensions were prepared with Milli-Q water. PANI-TiO_2 composites used as adsorbents were synthesized according to a previously reported procedure[47,48] reported in Section S1.

2.1 Adsorption ad release tests

Adsorption tests were performed at 25 °C and at controlled pH in a jacked reactor equipped with magnetic stirring. Tests were carried out on methyl orange (MO) aqueous solutions in a

concentration range from 10 to 600 ppm, at different pH values (3.0-4.0 range, adjusted by addition of HCl and NaOH solutions) and with PANI-TiO_2 suspension either 0.5 g/L or 2.5 g/L. Different types of water matrices were tested: milliQ water and aqueous solutions of several electrolytes (NaCl, Na_2SO_4, $MgCl_2$, $MgSO_4$, 0.01M cation concentration). The adsorbent was recovered by centrifugation. The amount of dye adsorbed and released in the supernatant solution was evaluated via UV-vis absorption at the maximum absorption wavelength (Shimadzu UV-2600).

Release tests were conducted by suspending the saturated adsorbent (after multiple adsorption tests on MO solutions in water) in NaOH solution (pH 9, 0.5 g adsorbent/L) at 25 °C under magnetic stirring. The regenerated material was readopted for further consecutive adsorption tests in acidic conditions.

Selectivity tests were performed on a mixture of 10 ppm MO and 10 ppm methylene blue (MB), using 2.5 g/L of adsorbent and a contact time of 10 min. Eight consecutive adsorption tests were performed without adjusting the pH nor adding new adsorbent, and then the dye release was conducted in an alkaline solution (pH 9 by NaOH, 1.0 g/L adsorbent dose, 25 °C, 10 min).

2.2 Photocatalytic tests

Photocatalytic tests were performed towards the degradation of MO, either in *ad hoc* prepared solutions and in solutions from released tests (as described in Section 2.1), with a concentration ranging from 10 to 50 ppm. Tests were carried out in different pH conditions and water matrices (ultrapure water and simulated tap water prepared according to a standard protocol[48]). Photocatalytic tests were performed in a jacketed reactor at 25 °C under magnetic stirring, in aerated conditions by O_2 bubbling and under UV irradiation. Commercial ZnO from Sigma Aldrich was adopted as photocatalyst: the physicochemical characteristics of the oxide are reported in Tab.S2. The oxide was preirradiated for 1h before the photocatalytic test, then 0.5 g/L of photocatalyst was suspended in the MO solution for 30 min in the dark to achieve adsorption-desorption equilibrium. UV irradiation was performed by a halogen lamp (Jelosil HG500 lamp, 320-400 nm, effective power density 30 mW/cm^2). Photolysis was also determined by separate tests. The dye disappearance was monitored by UV-vis spectroscopy measuring the intensity at the maximum absorption wavelength.

3. Results and Discussion

3.1 Optimization of the adsorption step

A PANI-TiO_2 composite was adopted as adsorbent for dye removal tests: the main physicochemical properties of this material are reported in Tab.S1. The hybrid photocatalytic synthetic procedure,

initiated by TiO_2, gives rise to a composite characterized by a relatively large surface area (almost 50 m^2/g, Fig.1b), high porosity in the mesoporous range (Fig.1c), and by a rod-like morphology of the PANI matrix, as highlighted by SEM images (Fig.1a). Elongated morphologies have been previously reported to be beneficial for pollutant adsorption by PANI materials[49].

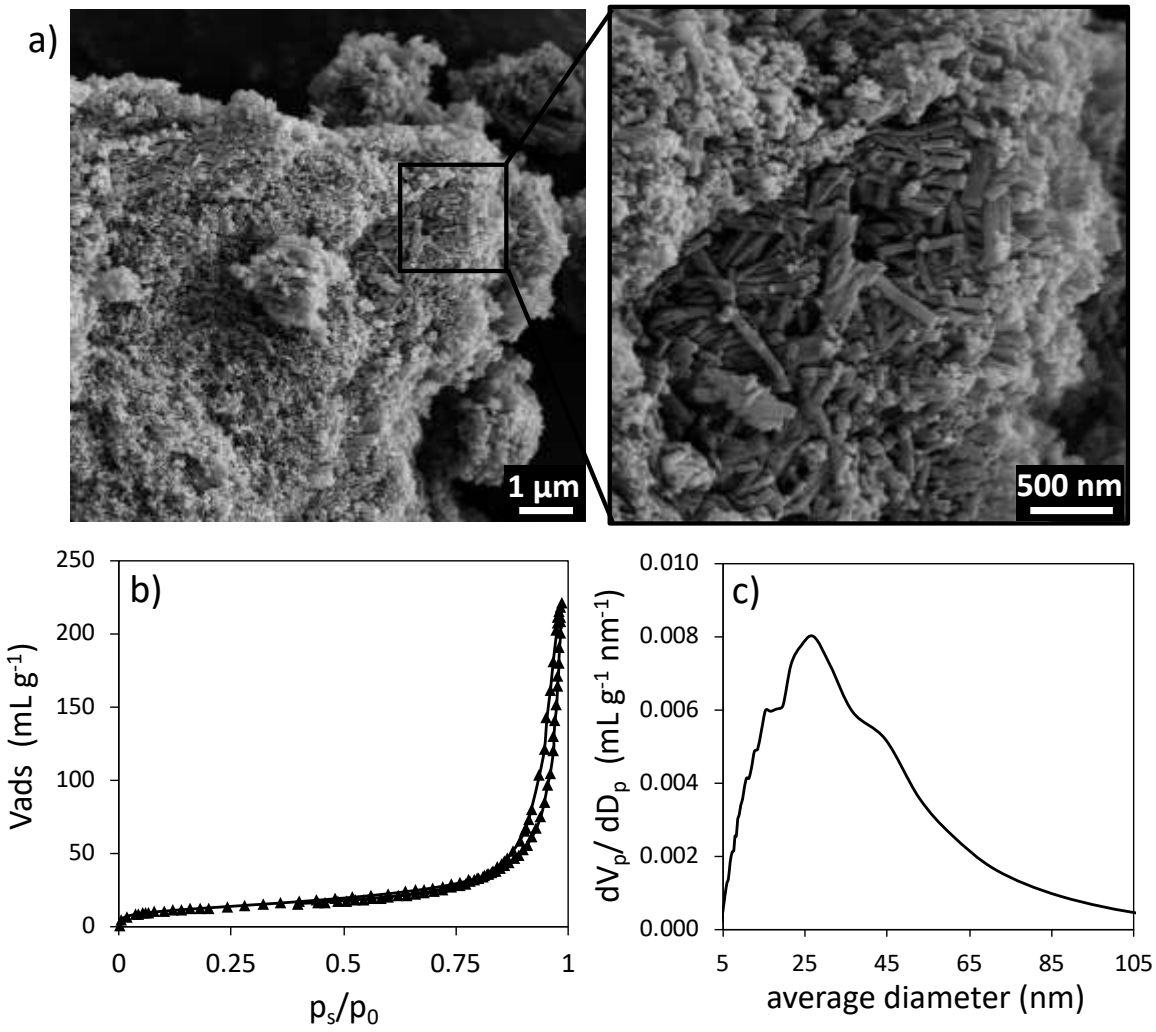

Fig.1. Morphology of PANI-TiO_2 adsorbent: a) SEM images, b) N_2 adsorption–desorption isotherm of N_2 in subcritical conditions and c) pore size distribution.

Firstly, PANI-based composites were tested towards the removal of an anionic dye, methyl orange (MO). The effect of initial MO concentrations on adsorption was studied by adsorption isotherms. It is indeed well known that the initial concentration represents a driving force to overcome mass transfer resistance between the adsorbent and the solution. Fig.S1 reports the adsorption isotherm of MO onto PANI-TiO_2 composite with 0.5 g/L adsorbent dose in a dye concentration range 10-200 ppm. Experimental data were fitted according to the Langmuir, Freundlich and Temkin isotherm

models (Section S2). By considering linear regressions (Fig.S1, inset), experimental data are best described by a Langmuir model.

The adsorption kinetics was also investigated. Fig.S2a reports an adsorption kinetic test performed with 0.5 g/L adsorbent in 100 ppm dye solution. MO uptake increased with the sorption time until equilibrium was reached between the solid adsorbent and solution. Data were fitted using Pseudo First Order (PSO), Pseudo Second Order (PSO), Intra-Particle Diffusion (IPD) and Elovich kinetic models (Section S3)[50]. On the grounds of correlation coefficients (Tab.S4), the model that best fit the experimental data was a pseudo-first-order kinetics (R^2=0.99526), with q_e=154 mg/g. The linearized IPD plot reported in Fig.S3 clearly shows two distinct linear regions, which on the grounds of the IPD model can be related to film diffusion and to the intra-particle diffusion stage, respectively.

In order to tailor the required contact time to achieve satisfactory dye removal, the adsorbent dose can be modulated to increase the easily accessible surface sites[23]. By increasing the adsorbent dose to 2.5 g/L, a very fast adsorption kinetics can be obtained even using highly concentrated dye solutions (600 ppm). As shown by Fig.S2b, 88% of the dye in solution was removed in just 1 min and equilibrium conditions (93%) were reached in less than 10 min.

The role of the solution pH was also investigated: this parameter is indeed well known to affect the sorption process by influencing both the ionization degree of the adsorbate and the adsorbent surface charge. Fig.2a reports the dye removal as a function of solution pH: higher dye uptakes are observed at pH values lower than 3.5, whereas dye removal drops at higher pH values. Further increases in pH lead to even lower adsorption (*vide infra*). These observations can be traced back to the pK_a of methyl orange (3.47) and the acid-base forms of polyaniline (Figs.S4-S5). Fig.3a shows a schematic representation of the interactions between PANI chains and MO molecules in different pH ranges. At pH values lower than the pK_a of MO (green arrow in Fig.3a), both π-π stacking between aromatic rings (red dotted line), electrostatic interactions between the $-SO_3^-$ and $-NH^+=$ groups (green dotted line) and H-bonds between -NH- groups (blue dotted line) can occur. By increasing the pH between MO pK_a and the adsorbent isoelectric point (yellow arrow in Fig.3a), H-bonds between PANI and MO are lost, while electrostatic and π-π interactions are still present. A further increase in pH leads to the deprotonation of PANI: in this scenario, where both MO and PANI are in their alkaline forms (red arrow in Fig.3a), only π- π interactions can occur between the polymer chains and the dye molecule. It must be noted that, at pH values higher than PANI-TiO_2 isoelectric point (*i.e.,* pH>4.8), the composite material is negatively charged, thus electrostatic repulsion occurs between the adsorbent and MO molecules (*vide infra*).

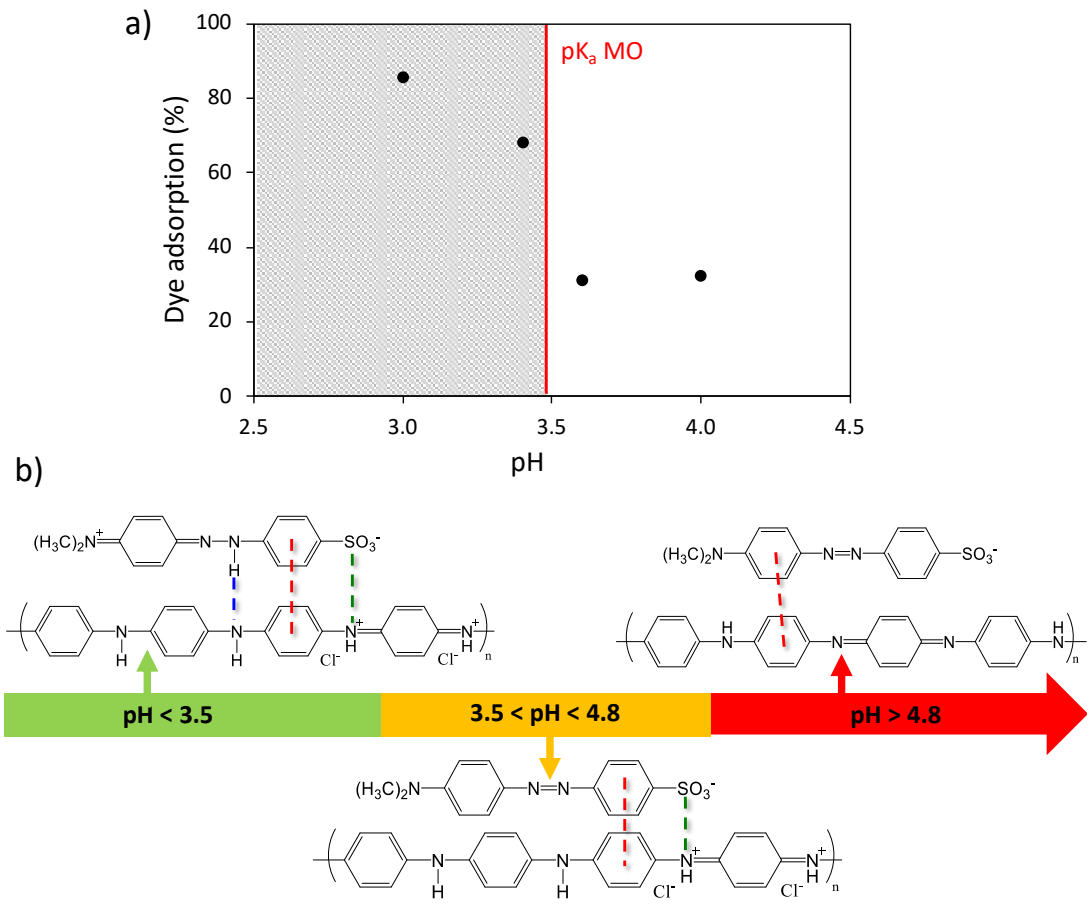

Fig.2. a) Role of pH on dye adsorption (0.5 g/L of adsorbent, 100 ppm MO solutions, 30 min); the pK_a of methyl orange is highlighted as a red vertical line. b) Schematic representation of the PANI-methyl orange interactions occurring in different pH ranges.

Besides the solution pH, the electrolyte content of the adsorbate solution can affect the adsorption properties via interfering with adsorbate-adsorbent electrostatic interactions[52]. This aspect is crucial for applying the PANI-TiO_2 adsorbent in complex water matrices. Therefore, the dye adsorption capacity of PANI-TiO_2 composite was tested in the presence of different electrolytes at constant concentration. Fig.2a,b shows the dependence of MO adsorption on the water matrix composition and the solution ionic strength. A slight decrease in MO removal was observed upon electrolyte addition, particularly in the case of monovalent ions (Fig.2a). Elecrolytes can indeed compete with the anionic dye for adsorption at the active sites by electrostatic interactions. No clear trends can be observed at increasing the solution ionic strength (Fig.2b). Nonetheless, in all the tested water matrices, the dye removal was always higher than 85%, thus proving the robustness of the PANI-TiO_2 adsorption capacity also in the presence of different electrolytes.

The pH sensitivity of adsorption equilibria of our adsorbent can be exploited to achieve pH-triggered desorption. Methyl orange release tests were optimized by varying the solution pH (pH 9-10), suspension temperature (25-80°C), release time (from 10 minutes to 24 hours) and adsorbent

concentration (0.5 g/L and 2.5 g/L). It should be noted that literature studies propose far more severe regeneration conditions in terms of acid/base concentrations[23,51] or the addition of organic solvents[52–57]. Results showed that, even in mild conditions and for short release time (0.5 mg/mL adsorbent, 30 min, 25°C, pH 9), the material released up to 60% of the adsorbed dye, which proved sufficient to restore the activity of the regenerated adsorbent to values fully comparable to the pristine adsorbent ((96±3)% and (92±3%), respectively). This release capacity can thus be exploited in order to regenerate the spent adsorbent after consecutive adsorption cycles. It should be noted that the presently adopted mild regeneration conditions make it easier to perform subsequent treatments on the released dye solution.

A key feature for the applicability of the present adsorption system to multi-pollutant wastewaters is its selectivity. The acid-base sensitivity of the adsorption process opens the door to the pH-driven selectivity towards anionic/cationic dyes. Here, adsorption tests were carried out on a mixture solution of cationic (MB) and anionic (MO) dyes. Fig.3c,d shows UV-visible spectra and pictures of the starting solution (green line) and of the same solution after adsorption (blue line). It is noteworthy that the peak of MO at 514 nm nearly disappears after adsorption, while the main peak of MB at 670 nm is almost unvaried. Fig.3e reports consecutive adsorption tests in the MB and MO mixed solution. A high degree of selectivity is observed towards the anionic dye due to the strong interactions (electrostatic, H-bond and π- π stacking) between MO and the PANI chains, while the cationic dye is repelled by same charge electrostatic interactions. The same procedure was repeated for 8 consecutive tests without adjusting the solution pH (Fig.3f) and without making up for any adsorbent loss. The average selectivity over the first 5 cycles was 93% and remained >68% in all consecutive runs (Fig.3f). A minor decrease in selectivity (both in terms of increased MB removal and decreased MO adsorption) could be observed only when the solution pH approached a value of 4.0. This result is expected based on the previously discussed role of solution pH on PANI adsorption features and could be further exploited to reverse the selectivity towards cationic dyes. Indeed, MB adsorption could be achieved by adopting an alkaline pH (84% MB removal using pH 9.0, 50 ppm MB, 10 min, 2.5 g/L adsorbent).

At the end of the selective adsorption tests for the removal of MO, the retrieved adsorbent was suspended in an alkaline solution (pH 9.0). Fig.3c,d show the UV-vis spectrum and photo of the release solution (orange line): while the peak of MO at 514 nm is clearly appreciable, no absorption peak ascribable to MB can be observed. The selectivity in the adsorption process coupled with the ability of the material to release the adsorbed molecule in mild condition, led to a selective MO recovery that could enable its recycling in a circular economy perspective.

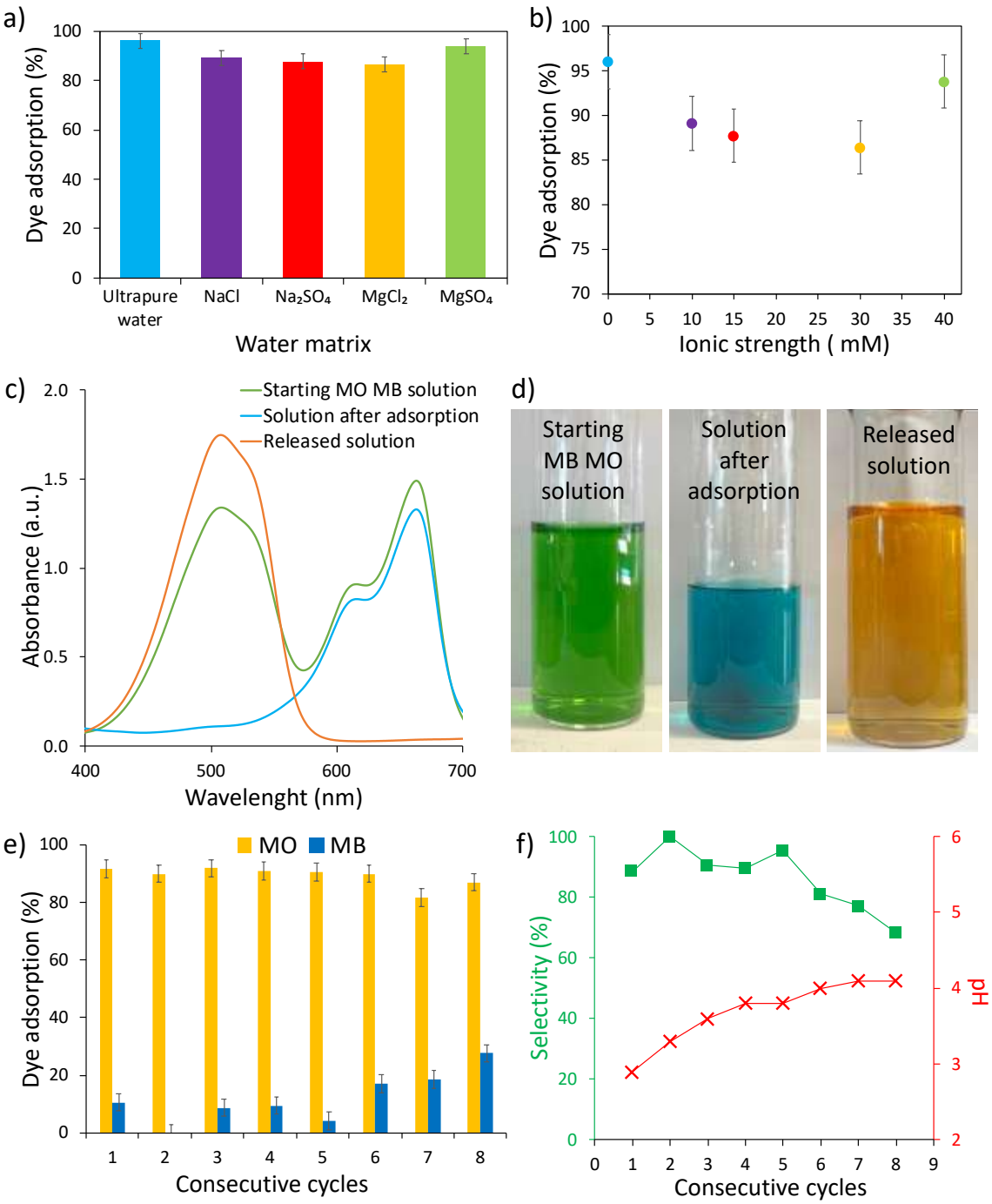

Fig.3. Dye adsorption percentage in function of a) type of water matrix, b) solution ionic strength; Conditions: 2.5 g/L of adsorbent; 50 ppm MO solutions in the presence of different electrolytes (0.01 M cation concentration), 30 min, pH 3.0). c) UV-vis spectra and d) photos of a mixture solution of 10 ppm MO and 10 ppm MB dyes as prepared, after selective adsorption and of the solution released by the adsorbent; e) Dye removal in consecutive selective adsorption tests and f) relative selectivity (green squares) and solution pH (red crosses).

3.2 Photocatalytic degradation of the released dye

Before discharge, leftover solutions need further treatment. In this respect, a separate photocatalytic test can be adopted to completely degrade recalcitrant dyes. Here we propose, as an example, the

photocatalytic treatment of the regeneration solution to show the simple implementation of the AOP step after the adsorption cycle in mild conditions.

In these regards, it must be considered that PANI-TiO_2 did not show any significant photoactivity under UV irradiation in water media. Therefore, in the present study, a commercial ZnO powder was adopted as photocatalyst. Zinc oxide is a large-band gap oxide semiconductor[58,59], which is attracted increasing interest from the scientific community[59,60]. This photocatalyst was here selected on the grounds of previous works[61–63] showing a higher photoactivity of ZnO in complex water matrices with respect to a benchmark TiO_2 samples. This observation was here confirmed by tests performed with MO solutions in different water matrices (ultrapure water and simulated tap water): as reported by Fig.S6, the presence of multiple electrolytes does not hinder ZnO photodegradation activity.

The role of the solution pH and starting dye concentration was also investigated. Fig.S7 reports photocatalytic degradation tests of MO by ZnO at neutral pH, as a function of the initial dye concentration. In all cases, dark adsorption is negligible (<10%). As expected, increasing the dye amount leads to longer degradation times. While 10 ppm solutions are completely degraded in ca. 60 min, 50 ppm solutions require more than 3 hours to remove the day completely. For the sake of comparison, adsorption tests could achieve the abatement of 50 ppm solutions in less than 10 min. In this respect, this selective and reversible adsorption system could also be proposed to quickly remove a pollutant of main concern from the effluent, while photocatalysis could be used to treat the solution obtained by the adsorbent regeneration containing only the target contaminant.

Fig.4a reports the effect of the solution pH on MO degradation: increasing the pH value to 9 has a marked detrimental effect on MO disappearance with respect to tests performed at neutral pH. This observation is in agreement with literature results[64], showing better performance of MO degradation by ZnO photocatalysts at neutral conditions with respect to acidic or alkaline environments. This dictates the importance of restoring a pH value close to neutrality after dye release before photocatalytic degradation.

Photocatalytic tests were also performed on the dye solution obtained upon release from nine adsorption tests of MO at 50 ppm. The final pH was neutralized using HCl addition and the concentration was adjusted to 15 ppm. Fig.4b reports the results in terms of dye degradation. For the sake of comparison, Fig.4b also shows the MO removal curves by photocatalysis and photolysis of *ad hoc* prepared MO solutions in ultrapure water with the same initial dye concentration (15 ppm) and solution pH.

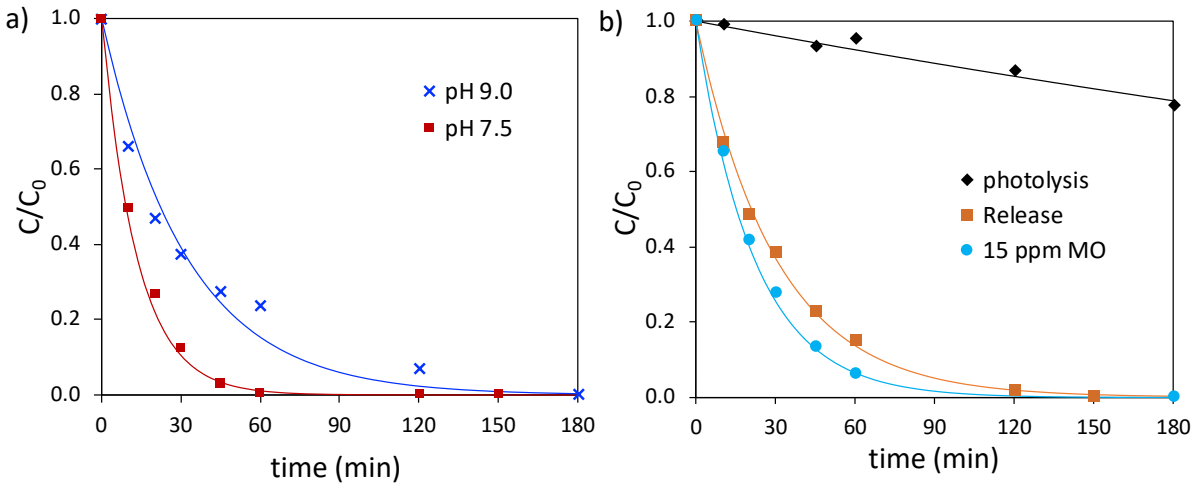

Fig.4. a) Photocatalytic tests performed with 10 ppm MO solutions at different pH values; b) Photocatalytic and photolytic tests of 15 ppm MO solutions at pH 7.5 compared to photocatalytic degradation of the MO released solution at the same starting MO concentration and pH. Data are fitted with pseudo-first order kinetic model.

Photolysis of MO in the adopted irradiation conditions is very low (<20% in 3 hours). Both tests in the presence of ZnO photocatalyst showed complete degradation of the dye molecule within 120 min. The test performed on the *ad hoc* prepared solution showed the fastest disappearance (k = (4.53±0.06)×10^{-2} min^{-1}) with respect to the photocatalytic abatement of the released solution (k = (3.31±0.04)×10^{-2} min^{-1}). This difference could be attributed to the presence of electrolytes or of traces of organic residues in the solution from the adsorbent regeneration. However, both tests resulted in >80% dye removal in 60 min, confirming the applicability of the photocatalytic approach for the treatment of the solution from the adsorbent regeneration.

4. Conclusions

In this work, adsorption and photocatalysis are coupled for the treatment of dye-containing waters.

A polyaniline-based adsorbent was adopted to achieve a reversible and selective removal of dyes: by modulating the adsorption pH, anionic or cationic dyes could be selectively adsorbed also in high concentrations and in multiple consecutive adsorption tests. Dye adsorption could also be performed in electrolyte solutions with different ionic strengths. The regeneration of the adsorbent and the concomitant controlled release of the adsorbed dye could be obtained in mild conditions by reversing the solution pH.

Thanks to the mild conditions adopted in the adsorption cycle, a photocatalytic post-treatment can be easily coupled to fully degrade any leftover contaminant. Here, the approach was demonstrated on the regeneration solution by using a commercial ZnO photocatalyst characterized by robustness in electrolyte-containing water matrices. The released dye solution, after pH adjustment, could be

photocatalytically treated, achieving a complete molecule disappearance with a photocatalytic performance only mildly affected compared to the treatment of the same dye concentration in ultrapure water.

In conclusion, the ease of regeneration of the PANI-based adsorbent reduces waste production by prolonging the useful life of the solid adsorbent. Moreover, the separation of multi-dye mixtures enables the selective recovery and potential reuse of raw materials. Finally, the simplified effluent composition allows performing a second photocatalytic step in a more efficient way to fully degrade the recalcitrant dye before discharge. Future studies will extend this approach to other dye molecules, as well as to other classes of charged pollutants, and to immobilized adsorbents and photocatalysts for easier recovery.

References

[1] A. Reghioua, D. Barkat, A.H. Jawad, A.S. Abdulhameed, A.A. Al-Kahtani, Z.A. ALOthman, Parametric optimization by Box–Behnken design for synthesis of magnetic chitosan-benzil/ZnO/Fe_3O_4 nanocomposite and textile dye removal, J. Environ. Chem. Eng. 9 (2021) 105166. https://doi.org/10.1016/j.jece.2021.105166.

[2] Z. Rahimi, A.A. Zinatizadeh, S. Zinadini, M. van Loosdrecht, A hydrophilic and antifouling nanofiltration membrane modified by citric acid functionalized tannic acid (CA-f-TA) nanocomposite for dye removal from biologically treated baker's yeast wastewater, J. Environ. Chem. Eng. 9 (2021) 104963. https://doi.org/10.1016/j.jece.2020.104963.

[3] S.K. Panda, I. Aggarwal, H. Kumar, L. Prasad, A. Kumar, A. Sharma, D.-V.N. Vo, D. Van Thuan, V. Mishra, Magnetite nanoparticles as sorbents for dye removal: a review, Environ. Chem. Lett. 19 (2021) 2487–2525. https://doi.org/10.1007/s10311-020-01173-9.

[4] J. Xu, X. Zheng, Z. Feng, Z. Lu, Z. Zhang, W. Huang, Y. Li, D. Vuckovic, Y. Li, S. Dai, G. Chen, K. Wang, H. Wang, J.K. Chen, W. Mitch, Y. Cui, Organic wastewater treatment by a single-atom catalyst and electrolytically produced H2O2, Nat. Sustain. 4 (2021) 233–241. https://doi.org/10.1038/s41893-020-00635-w.

[5] O. Garcia-Rodriguez, E. Mousset, H. Olvera-Vargas, O. Lefebvre, Electrochemical treatment of highly concentrated wastewater: A review of experimental and modeling approaches from lab- to full-scale, Crit. Rev. Environ. Sci. Technol. 52 (2022) 240–309. https://doi.org/10.1080/10643389.2020.1820428.

[6] S. Mishra, L. Cheng, A. Maiti, The utilization of agro-biomass/byproducts for effective bio-removal of dyes from dyeing wastewater: A comprehensive review, J. Environ. Chem. Eng. 9 (2021) 104901. https://doi.org/10.1016/j.jece.2020.104901.

[7] A. Yadav, P. Sharma, A.B. Panda, V.K. Shahi, Photocatalytic TiO_2 incorporated PVDF-co-HFP UV-cleaning mixed matrix membranes for effective removal of dyes from synthetic wastewater system via membrane distillation, J. Environ. Chem. Eng. 9 (2021) 105904. https://doi.org/10.1016/j.jece.2021.105904.

[8] V. Katheresan, J. Kansedo, S.Y. Lau, Efficiency of various recent wastewater dye removal methods: A review, J. Environ. Chem. Eng. 6 (2018) 4676–4697. https://doi.org/10.1016/j.jece.2018.06.060.

[9] P. Chanikya, P. V. Nidheesh, D. Syam Babu, A. Gopinath, M. Suresh Kumar, Treatment of dyeing wastewater by combined sulfate radical based electrochemical advanced oxidation and electrocoagulation processes, Sep. Purif. Technol. 254 (2021) 117570. https://doi.org/10.1016/j.seppur.2020.117570.

[10] K. Sarayu, S. Sandhya, Current Technologies for Biological Treatment of Textile Wastewater–A Review, Appl. Biochem. Biotechnol. 167 (2012) 645–661. https://doi.org/10.1007/s12010-012-9716-6.

[11] P.V. Nidheesh, R. Gandhimathi, S.T. Ramesh, Degradation of dyes from aqueous solution by Fenton processes: a review, Environ. Sci. Pollut. Res. 20 (2013) 2099–2132. https://doi.org/10.1007/s11356-012-1385-z.

[12] G. Gnanapragasam, M. Senthilkumar, V. Arutchelvan, T. Velayutham, S. Nagarajan, Bio-kinetic analysis on treatment of textile dye wastewater using anaerobic batch reactor, Bioresour. Technol. 102 (2011) 627–632. https://doi.org/10.1016/j.biortech.2010.08.012.

[13] F. Mcyotto, Q. Wei, D.K. Macharia, M. Huang, C. Shen, C.W.K. Chow, Effect of dye structure on color removal efficiency by coagulation, Chem. Eng. J. 405 (2021) 126674. https://doi.org/10.1016/j.cej.2020.126674.

[14] V.K. Gupta, D. Pathania, N.C. Kothiyal, G. Sharma, Polyaniline zirconium (IV) silicophosphate nanocomposite for remediation of methylene blue dye from waste water, J. Mol. Liq. 190 (2014) 139–145. https://doi.org/10.1016/j.molliq.2013.10.027.

[15] C. Yang, W. Xu, Y. Nan, Y. Wang, Y. Hu, C. Gao, X. Chen, Fabrication and characterization of a high performance polyimide ultrafiltration membrane for dye removal, J. Colloid Interface Sci. 562 (2020) 589–597. https://doi.org/10.1016/j.jcis.2019.11.075.

[16] S. Selvakumar, R. Manivasagan, K. Chinnappan, Biodegradation and decolourization of textile dye wastewater using Ganoderma lucidum, 3 Biotech. 3 (2013) 71–79. https://doi.org/10.1007/s13205-012-0073-5.

[17] M. Senthilkumar, G. Gnanapragasam, V. Arutchelvan, S. Nagarajan, Treatment of textile dyeing wastewater using two-phase pilot plant UASB reactor with sago wastewater as co-

substrate, Chem. Eng. J. 166 (2011) 10–14. https://doi.org/10.1016/j.cej.2010.07.057.

[18] P. Suresh, J.J. Vijaya, L.J. Kennedy, Photocatalytic degradation of textile-dyeing wastewater by using a microwave combustion-synthesized zirconium oxide supported activated carbon, Mater. Sci. Semicond. Process. 27 (2014) 482–493. https://doi.org/10.1016/j.mssp.2014.06.050.

[19] K. Haitham, S. Razak, M.A. Nawi, Kinetics and isotherm studies of methyl orange adsorption by a highly recyclable immobilized polyaniline on a glass plate, Arab. J. Chem. 12 (2019) 1595–1606. https://doi.org/10.1016/j.arabjc.2014.10.010.

[20] M. Afshari, M. Dinari, H. Moradi, Z. Noori, Polyaniline/sulfonated-covalent organic polymer nanocomposite: Structural and dye adsorption properties, Polym. Adv. Technol. 31 (2020) 2433–2442. https://doi.org/10.1002/pat.4959.

[21] E.S. Mansor, H. Ali, A. Abdel-Karim, Efficient and reusable polyethylene oxide/polyaniline composite membrane for dye adsorption and filtration, Colloid Interface Sci. Commun. 39 (2020) 100314. https://doi.org/10.1016/j.colcom.2020.100314.

[22] J. Shen, S. Shahid, I. Amura, A. Sarihan, M. Tian, E.A. Emanuelsson, Enhanced adsorption of cationic and anionic dyes from aqueous solutions by polyacid doped polyaniline, Synth. Met. 245 (2018) 151–159. https://doi.org/10.1016/j.synthmet.2018.08.015.

[23] M. Bhaumik, R.I. McCrindle, A. Maity, S. Agarwal, V.K. Gupta, Polyaniline nanofibers as highly effective re-usable adsorbent for removal of reactive black 5 from aqueous solutions, J. Colloid Interface Sci. 466 (2016) 442–451. https://doi.org/10.1016/j.jcis.2015.12.056.

[24] T. Robinson, G. McMullan, R. Marchant, P. Nigam, Remediation of dyes in textile effluent: a critical review on current treatment technologies with a proposed alternative, Bioresour. Technol. 77 (2001) 247–255. https://doi.org/10.1016/S0960-8524(00)00080-8.

[25] L.S. Mendieta-Rodríguez, L.M. González-Rodríguez, J.J. Alcaraz-Espinoza, A.E. Chávez-Guajardo, J.C. Medina-Llamas, Synthesis and characterization of a polyurethane-polyaniline macroporous foam material for methyl orange removal in aqueous media, Mater. Today Commun. 26 (2021) 102155. https://doi.org/10.1016/j.mtcomm.2021.102155.

[26] V. Yönten, N.K. Sanyürek, M.R. Kivanç, A thermodynamic and kinetic approach to adsorption of methyl orange from aqueous solution using a low cost activated carbon prepared from Vitis vinifera L., Surfaces and Interfaces. 20 (2020) 100529. https://doi.org/10.1016/j.surfin.2020.100529.

[27] K. Jahan, S. Tyeb, N. Kumar, V. Verma, Bacterial Cellulose-Polyaniline Porous Mat for Removal of Methyl Orange and Bacterial Pathogens from Potable Water, J. Polym. Environ. 29 (2021) 1257–1270. https://doi.org/10.1007/s10924-020-01947-w.

[28] E. Pargoletti, V. Pifferi, L. Falciola, G. Facchinetti, A. Re Depaolini, E. Davoli, M. Marelli, G. Cappelletti, A detailed investigation of MnO_2 nanorods to be grown onto activated carbon. High efficiency towards aqueous methyl orange adsorption/degradation, Appl. Surf. Sci. 472 (2019) 118–126. https://doi.org/10.1016/j.apsusc.2018.03.170.

[29] Y. Liu, X. He, Y. Fu, D.D. Dionysiou, Degradation kinetics and mechanism of oxytetracycline by hydroxyl radical-based advanced oxidation processes, Chem. Eng. J. 284 (2016) 1317–1327. https://doi.org/10.1016/j.cej.2015.09.034.

[30] R.C. Asha, M.A. Vishnuganth, N. Remya, N. Selvaraju, M. Kumar, Livestock Wastewater Treatment in Batch and Continuous Photocatalytic Systems: Performance and Economic Analyses, Water. Air. Soil Pollut. 226 (2015). https://doi.org/10.1007/s11270-015-2396-4.

[31] V. Homem, L. Santos, Degradation and removal methods of antibiotics from aqueous matrices – A review, J. Environ. Manage. 92 (2011) 2304–2347. https://doi.org/10.1016/j.jenvman.2011.05.023.

[32] H. Barndõk, D. Hermosilla, C. Han, D.D. Dionysiou, C. Negro, Á. Blanco, Degradation of 1,4-dioxane from industrial wastewater by solar photocatalysis using immobilized NF-TiO2 composite with monodisperse TiO_2 nanoparticles, Appl. Catal. B Environ. 180 (2016) 44–52. https://doi.org/10.1016/j.apcatb.2015.06.015.

[33] M.R.D. Khaki, M.S. Shafeeyan, A.A.A. Raman, W.M.A.W. Daud, Application of doped photocatalysts for organic pollutant degradation - A review, J. Environ. Manage. 198 (2017) 78–94. https://doi.org/10.1016/j.jenvman.2017.04.099.

[34] M. Melchionna, P. Fornasiero, Updates on the Roadmap for Photocatalysis, ACS Catal. 10 (2020) 5493–5501. https://doi.org/10.1021/acscatal.0c01204.

[35] A. Colombo, G. Cappelletti, S. Ardizzone, I. Biraghi, C.L. Bianchi, D. Meroni, C. Pirola, F. Spadavecchia, Bisphenol A endocrine disruptor complete degradation using TiO_2 photocatalysis with ozone, Environ. Chem. Lett. 10 (2012) 55–60. https://doi.org/10.1007/s10311-011-0328-0.

[36] S.K. Loeb, P.J.J. Alvarez, J.A. Brame, E.L. Cates, W. Choi, J. Crittenden, D.D. Dionysiou, Q. Li, G. Li-Puma, X. Quan, D.L. Sedlak, T. David Waite, P. Westerhoff, J.-H. Kim, The Technology Horizon for Photocatalytic Water Treatment: Sunrise or Sunset?, Environ. Sci. Technol. 53 (2019) 2937–2947. https://doi.org/10.1021/acs.est.8b05041.

[37] I. Dalmázio, M.O. Almeida, R. Augusti, T.M.A. Alves, Monitoring the degradation of tetracycline by ozone in aqueous medium via atmospheric pressure ionization mass spectrometry, J. Am. Soc. Mass Spectrom. 18 (2007) 679–687. https://doi.org/10.1016/j.jasms.2006.12.001.

[38] V. Maroga Mboula, V. Héquet, Y. Gru, R. Colin, Y. Andrès, Assessment of the efficiency of photocatalysis on tetracycline biodegradation, J. Hazard. Mater. 209–210 (2012) 355–364. https://doi.org/10.1016/j.jhazmat.2012.01.032.

[39] J.J. Rueda-Marquez, I. Levchuk, P. Fernández Ibañez, M. Sillanpää, A critical review on application of photocatalysis for toxicity reduction of real wastewaters, J. Clean. Prod. 258 (2020) 120694. https://doi.org/10.1016/j.jclepro.2020.120694.

[40] L. Rimoldi, D. Meroni, E. Falletta, V. Pifferi, L. Falciola, G. Cappelletti, S. Ardizzone, Emerging pollutant mixture mineralization by TiO_2 photocatalysts. The role of the water medium, Photochem. Photobiol. Sci. 16 (2017) 60–66. https://doi.org/10.1039/C6PP00214E.

[41] M. Krivec, R. Dillert, D.W. Bahnemann, A. Mehle, J. Štrancar, G. Dražić, The nature of chlorine-inhibition of photocatalytic degradation of dichloroacetic acid in a TiO_2-based microreactor, Phys. Chem. Chem. Phys. 16 (2014) 14867. https://doi.org/10.1039/c4cp01043d.

[42] N. Wang, J. Li, W. Lv, J. Feng, W. Yan, RSC Advances excellent adsorption performance on acid red G, RSC Adv. 5 (2015) 21132–21141. https://doi.org/10.1039/C4RA16910G.

[43] C. Della Pina, M.A. De Gregorio, L. Clerici, P. Dellavedova, E. Falletta, Polyaniline (PANI): an innovative support for sampling and removal of VOCs in air matrices, J. Hazard. Mater. 344 (2018) 308–315. https://doi.org/10.1016/j.jhazmat.2017.10.012.

[44] J. Zhang, J. Han, M. Wang, R. Guo, Fe_3O_4/PANI/MnO_2 core-shell hybrids as advanced adsorbents for heavy metal ions, J. Mater. Chem. A. 5 (2017) 4058–4066. https://doi.org/10.1039/c6ta10499a.

[45] M. Saad, H. Tahir, J. Khan, U. Hameed, A. Saud, Synthesis of polyaniline nanoparticles and their application for the removal of Crystal Violet dye by ultrasonicated adsorption process based on Response Surface Methodology, Ultrason. Sonochem. 34 (2017) 600–608. https://doi.org/10.1016/j.ultsonch.2016.06.022.

[46] W. Lyu, M. Yu, J. Feng, W. Yan, Highly crystalline polyaniline nanofibers coating with low-cost biomass for easy separation and high efficient removal of anionic dye ARG from aqueous solution, Appl. Surf. Sci. 458 (2018) 413–424. https://doi.org/10.1016/j.apsusc.2018.07.074.

[47] C. Cionti, C. Della Pina, D. Meroni, E. Falletta, S. Ardizzone, Triply green polyaniline: UV irradiation-induced synthesis of a highly porous PANI/TiO_2 composite and its application in dye removal, Chem. Commun. 54 (2018) 10702–10705. https://doi.org/10.1039/C8CC04745F.

[48] C. Cionti, C. Della Pina, D. Meroni, E. Falletta, S. Ardizzone, Photocatalytic and Oxidative

Synthetic Pathways for Highly Efficient PANI-TiO_2 Nanocomposites as Organic and Inorganic Pollutant Sorbents, Nanomaterials. 10 (2020) 441. https://doi.org/10.3390/nano10030441.

[49] J. Stejskal, Interaction of conducting polymers, polyaniline and polypyrrole, with organic dyes: polymer morphology control, dye adsorption and photocatalytic decomposition, Chem. Pap. 74 (2020) 1–54. https://doi.org/10.1007/s11696-019-00982-9.

[50] G.W. Hajjumba, S. Emik, S. and Ö. Aydin, Modelling of Adsorption Kinetic Processes - Errors , Theory and, Intech Open. (2018) 0–19.

[51] Y. Liu, Y. Zhao, W. Cheng, T. Zhang, Targeted reclaiming cationic dyes from dyeing wastewater with a dithiocarbamate-functionalized material through selective adsorption and efficient desorption, J. Colloid Interface Sci. 579 (2020) 766–777. https://doi.org/10.1016/j.jcis.2020.06.083.

[52] S. Tang, D. Xia, Y. Yao, T. Chen, J. Sun, Y. Yin, W. Shen, Y. Peng, Dye adsorption by self-recoverable, adjustable amphiphilic graphene aerogel, J. Colloid Interface Sci. 554 (2019) 682–691. https://doi.org/10.1016/j.jcis.2019.07.041.

[53] F. Zhao, E. Repo, D. Yin, Y. Meng, S. Jafari, M. Sillanpää, EDTA-Cross-Linked β-Cyclodextrin: An Environmentally Friendly Bifunctional Adsorbent for Simultaneous Adsorption of Metals and Cationic Dyes, Environ. Sci. Technol. 49 (2015) 10570–10580. https://doi.org/10.1021/acs.est.5b02227.

[54] Z. Wu, H. Zhong, X. Yuan, H. Wang, L. Wang, X. Chen, G. Zeng, Y. Wu, Adsorptive removal of methylene blue by rhamnolipid-functionalized graphene oxide from wastewater, Water Res. 67 (2014) 330–344. https://doi.org/10.1016/j.watres.2014.09.026.

[55] X. Dai, S. Zhang, G.I.N. Waterhouse, H. Fan, S. Ai, Recyclable polyvinyl alcohol sponge containing flower-like layered double hydroxide microspheres for efficient removal of As(V) anions and anionic dyes from water, J. Hazard. Mater. 367 (2019) 286–292. https://doi.org/10.1016/j.jhazmat.2018.12.092.

[56] S. Ranote, D. Kumar, S. Kumari, R. Kumar, G.S. Chauhan, V. Joshi, Green synthesis of Moringa oleifera gum-based bifunctional polyurethane foam braced with ash for rapid and efficient dye removal, Chem. Eng. J. 361 (2019) 1586–1596. https://doi.org/10.1016/j.cej.2018.10.194.

[57] L. Zhou, C. Gao, W. Xu, Magnetic Dendritic Materials for Highly Efficient Adsorption of Dyes and Drugs, ACS Appl. Mater. Interfaces. 2 (2010) 1483–1491. https://doi.org/10.1021/am100114f.

[58] D. Meroni, C. Gasparini, A. Di Michele, S. Ardizzone, C.L. Bianchi, Ultrasound-assisted

synthesis of ZnO photocatalysts for gas phase pollutant remediation: Role of the synthetic parameters and of promotion with WO_3, Ultrason. Sonochem. 66 (2020) 105119. https://doi.org/10.1016/j.ultsonch.2020.105119.

[59] Y.K. Mishra, R. Adelung, ZnO tetrapod materials for functional applications, Mater. Today. 21 (2018) 631–651. https://doi.org/10.1016/j.mattod.2017.11.003.

[60] N. Wiesmann, W. Tremel, J. Brieger, Zinc oxide nanoparticles for therapeutic purposes in cancer medicine, J. Mater. Chem. B. 8 (2020) 4973–4989. https://doi.org/10.1039/d0tb00739k.

[61] D. Meroni, C.L. Bianchi, D.C. Boffito, G. Cerrato, A. Bruni, M. Sartirana, E. Falletta, Piezo-enhanced photocatalytic diclofenac mineralization over ZnO, Ultrason. Sonochem. 75 (2021) 105615. https://doi.org/10.1016/j.ultsonch.2021.105615.

[62] S. Mostoni, V. Pifferi, L. Falciola, D. Meroni, E. Pargoletti, E. Davoli, G. Cappelletti, Tailored routes for home-made Bi-doped ZnO nanoparticles. Photocatalytic performances towards o-toluidine, a toxic water pollutant, J. Photochem. Photobiol. A Chem. 332 (2017). https://doi.org/10.1016/j.jphotochem.2016.10.003.

[63] G. Cappelletti, V. Pifferi, S. Mostoni, L. Falciola, C. Di Bari, F. Spadavecchia, D. Meroni, E. Davoli, S. Ardizzone, Hazardous o-toluidine mineralization by photocatalytic bismuth doped ZnO slurries, Chem. Commun. 51 (2015) 10459–10462. https://doi.org/10.1039/C5CC02620B.

[64] S. Abbasi, M. Hasanpour, The effect of pH on the photocatalytic degradation of methyl orange using decorated ZnO nanoparticles with SnO_2 nanoparticles, J. Mater. Sci. Mater. Electron. 28 (2017) 1307–1314. https://doi.org/10.1007/s10854-016-5660-5.